PHYSICAL REVIEW D **78,** 104003 (2008)

Phantom stars and topology change

Andrew DeBenedictis[*]
Pacific Institute for the Mathematical Sciences, Simon Fraser University Site and Department of Physics, Simon Fraser University Burnaby, British Columbia, V5A IS6, Canada

Remo Garattini[+]
Università degli Studi di Bergamo, Facoltà di Ingegneria, Viale Marconi 5, 24044 Dalmine (Bergamo) ITALY and INFN - Sezione di Milano, Via Celoria 16, Milan, Italy

Francisco S. N. Lobo[‡]
Institute of Cosmology & Gravitation, University of Portsmouth, Portsmouth PO1 2EG, UK and Centro de Astronomia e Astrofísica da Universidade de Lisboa, Campo Grande, Ed. C8 1749-016 Lisboa, Portugal
(Received 6 August 2008; published 5 November 2008)

In this work, we consider time-dependent dark-energy star models, with an evolving parameter ω crossing the phantom divide $\omega = -1$. Once in the phantom regime, the null energy condition is violated, which physically implies that the negative radial pressure exceeds the energy density. Therefore, an enormous negative pressure in the center may, in principle, imply a topology change, consequently opening up a tunnel and converting the dark-energy star into a wormhole. The criteria for this topology change are discussed and, in particular, we consider a Casimir energy approach involving quasilocal energy difference calculations that may reflect or measure the occurrence of a topology change. We denote these exotic geometries consisting of dark-energy stars (in the phantom regime) and phantom wormholes as *phantom stars*. The final product of this topological change, namely, phantom wormholes, have far-reaching physical and cosmological implications, as in addition to being used for interstellar shortcuts, an absurdly advanced civilization may manipulate these geometries to induce closed timelike curves, consequently violating causality.

DOI: 10.1103/PhysRevD.78.104003 PACS numbers: 04.20.Jb, 04.40.Dg, 97.10.−q

I. INTRODUCTION

Recent high-precision observational data have confirmed that the Universe is undergoing a phase of accelerated expansion [1]. Several candidates, responsible for this expansion, have been proposed in the literature, in particular, dark-energy models (see Ref. [2] for a review) and modified gravity (e.g., see Ref. [3] for recent reviews). In particular, the former models are fundamental candidates, in which a simple way to parameterize the dark energy is by an equation of state of the form $\omega \equiv p/\rho$, where p is the spatially homogeneous pressure and ρ is the dark-energy density. A value of $\omega < -1/3$ is required for cosmic expansion, and $\omega = -1$ corresponds to a cosmological constant. A specific exotic form of dark energy denoted phantom energy, with $\omega < -1$, has also been proposed [4], and possesses peculiar properties, such as the violation of the null energy condition (NEC) and the energy density increases to infinity in a finite time [4], at which point the size of the Universe blows up in a finite time, which is known as the Big Rip. In this context, the violation of the NEC presents us with a natural scenario for the existence of traversable wormholes, and indeed it has been shown that these exotic geometries can be supported by phantom energy [5,6]. It is also interesting to note that recent fits to supernovae, cosmic microwave background radiation, and weak gravitational lensing data probably favor an evolving equation of state, with the parameter crossing the phantom divide $\omega = -1$ [7].

Despite the fact that the dark-energy equation of state represents a spatially homogeneous cosmic fluid and is assumed not to cluster, it is possible that inhomogeneities may arise due to gravitational instabilities. More precisely, although the equation of state leading to the acceleration of the Universe on large scales is an average equation of state corresponding to a background fluid, it is possible that dark-energy condensates may possibly originate from density fluctuations in the cosmological background, resulting in the nucleation through the respective density perturbations. Despite the fact that once in the dark-energy regime the material system becomes gravitationally repulsive, we may consider the possibility of the formation of a matter system that originally obeys all the energy conditions. Cosmological observations do not rule out, and in some studies favor, an evolving equation of state for the dark energy. It is therefore quite possible that what we know as dark energy today has evolved from a more benign fluid. An over density of this fluid could in principle commence a collapse into a star that at late times crosses the phantom divide in its interior. Such a model is presented in

[*]adebened@sfu.ca
[+]Remo.Garattini@unibg.it
[‡]francisco.lobo@port.ac.uk

 © 2008 The American Physical Society

Sec. III C. We also point out that even in the case of a dark-energy fluid, there is no definite resolution to the debate of clustering scales. This is mainly due to nonlinearity, especially in the vein of dark energy interacting with ordinary fluids. It may also be possible to glean some information on the cosmological dark matter by studying certain properties of such gravitational condensates. (See [8] and references therein for comments on these issues.) In this context, a number of inhomogeneous solutions have been the object of analysis, such as the phantom wormholes [5,6] mentioned above, dark-energy stars [9], and other structures such as condensates supported by the generalized Chaplygin gas [10], which possibly arise from density fluctuations in the generalized Chaplygin gas background, and condensed structures supported by the van der Waals equation of state [11]. In a recent paper [12], it was also shown that the 4D Einstein-Klein-Gordon equations with a phantom scalar field possess nonsingular, spherically symmetry solutions, although a stability analysis on these solutions indicates they are unstable.

The dark-energy star models are also a generalization of a new emerging picture for an alternative final state of gravitational collapse, namely, the gravastar (*gravitational vacuum star*) models. The latter proposed by Mazur and Mottola [13], has an effective phase transition at/near where the event horizon is expected to form, and the interior is replaced by a de Sitter condensate. The latter is then matched to a thick layer, with an equation of state given by $p = \rho$, which is in turn matched to an exterior Schwarzschild solution. The issue of gravastars has been extensively analyzed in the literature, and we refer the reader to Refs. [14,15]. The generalization of the gravastar picture is considered by matching an interior solution governed by the dark-energy equation of state $\omega \equiv p/\rho < -1/3$ to an exterior Schwarzschild vacuum solution at a junction interface [9]. The dynamical stability of the transition layer was also explored, and it was found that large stability regions exist that are sufficiently close to where the event horizon is expected to form, so that it was argued that it would be difficult to distinguish the exterior geometry of the dark-energy stars from an astrophysical black hole. Thus, these alternative models do not possess a singularity at the origin and have no event horizon, as its rigid surface is located at a radius slightly greater than the Schwarzschild radius. This restriction arises from the observed lack of energy emission due to surface collisions of infalling material in suspected black hole systems. In fact, although evidence for the existence of black holes is very convincing, a certain amount of scepticism regarding the physical reality of event horizons is still encountered, and it has been argued that despite the fact that observational data do indeed provide strong arguments in favor of event horizons, they cannot fundamentally prove their existence [16].

As mentioned above, recent fits to observational data probably favor an evolving equation of state, with the dark-energy parameter crossing the phantom divide $\omega = -1$ [7]. Motivated by this fact, in a rather speculative scenario one may theoretically consider the existence of a dark-energy star, with an evolving parameter starting out in the range $-1 < \omega < -1/3$, and crossing the phantom divide $\omega = -1$. Once in the phantom regime, the null energy condition is violated, which physically implies that the negative radial pressure exceeds the energy density. Therefore, an enormous negative pressure in the center may, in principle, imply a topology change, consequently opening up a tunnel, and converting the dark-energy star into a wormhole [9,17]. One may assume that the topology change may occur at approximately the Planck length scales, and once created may be self-sustained as shown in Ref. [18]. In fact, the change in topology is an extremely subtle issue, as in general relativity these changes probably entail spacetime singularities. However, at the Planck length scales quantum gravity effects dominate and spacetime undergoes a deep and rapid transformation in its structure, probably producing a multiply-connected quantum foam structure [19,20]. It was suggested in Ref. [17] that one could imagine an absurdly advanced civilization [21] pulling a wormhole from this submicroscopic spacetime quantum foam and enlarging it to macroscopic dimensions. However, in a more plausible scenario, the possibility that inflation might provide a natural mechanism for the enlargement of such wormholes to macroscopic size was explored [22]. In this work, we outline the theoretical difficulties associated to the change in topology and present a method based on the Casimir energy approach. Although it is still unsure if this method confirms a topology change, it is extremely useful as the quasilocal energy difference calculation may reflect or measure the occurrence of a change in topology. Other concepts of topology changing spacetimes have been studied. For instance, using semiclassical and Morse-index methods in Ref. [23], higher order back-reaction terms due to fluctuations of gauge fields in the vicinity of a black hole may result in the formation of a wormholelike object [24], and more recently an approach based on a Ricci flow may result in quantum wormholes [25].

Once the topology change has occurred, with the respective opening of a tunnel, then the dark-energy star has been converted into a wormhole supported by phantom energy. As mentioned above, it has recently been shown that traversable wormholes may, in principle, be supported by phantom energy [5,6], which apart from being used as interstellar shortcuts, may induce closed timelike curves with the associated causality violations [26,27]. Particularly interesting solutions have been found [6], and by using the ''volume integral quantifier,'' it was found that these wormhole geometries are, in principle, sustained by arbitrarily small amounts of averaged null energy condition violating phantom energy. A complementary approach was traced out in [5], by considering specific

choices for the distribution of the energy density threading the wormhole. Recently, 4D static wormhole solutions supported by two interacting phantom fields were found as well [28]. Despite the fact that traversable wormholes violate the NEC in general relativity (see Ref. [29] for a recent review), it has been shown that the stress-energy tensor profile may satisfy the energy conditions in the throat neighborhood in dynamic wormholes (see Ref. [30] and references therein) and in certain alternative theories to general relativity [31]. Perhaps not so appealing, one could denote these exotic geometries consisting of dark-energy stars (in the phantom regime) and phantom wormholes as *phantom stars*. We would like to state our agnostic position relative to the existence of dark-energy stars and phantom wormholes, or for that matter of phantom stars. However, it is important to understand their general properties and characteristics, and we emphasize that the presence of a dark-energy fluid permeating the Universe makes the study of dark-energy condensates a physically relevant endeavor.

This paper is organized in the following manner: In Sec. II, we briefly review static dark-energy stars, followed by a deduction of general solutions of time-dependent spacetimes. In Sec. III, specific time-dependent dark-energy solutions are outlined; in particular, we present the specific cases of a constant energy density, the Tolman-Matese-Whitman mass function solution, and a class of models with a nonzero energy flux term, which form from gravitational collapse. In Sec. IV, we describe the theoretical difficulties associated with changes in topology and present in some detail specific methods used in the literature, namely, a Casimir energy approach involving quasilocal energy difference calculations that may reflect or measure the occurrence of a topology change. In Sec. V, we conclude.

II. TIME-DEPENDENT DARK-ENERGY STARS

A. Static spacetime

In this section, we provide a brief outline of the mathematical models of static and spherically symmetric dark-energy stars considered in Ref. [9]. Consider the following time-independent line element, in curvature coordinates, representing a dark-energy star

$$ds^2 = -e^{2\alpha(r)}dt^2 + \frac{dr^2}{1-2m(r)/r} + r^2(d\theta^2 + \sin^2\theta d\phi^2), \tag{1}$$

where $\alpha(r)$ and $m(r)$ are arbitrary functions of the radial coordinate, r. The function $m(r)$ can be interpreted as the quasilocal mass, and is denoted as the mass function [9]. The factor $\alpha(r)$ is the "gravity profile" and is related to the locally measured acceleration due to gravity, through the following relationship: $\mathcal{A} = \sqrt{1-2m(r)/r}\alpha'(r)$ [9,11], where the prime denotes a derivative with respect to the radial coordinate r. The convention used is that $\alpha'(r)$ is positive for an inwardly gravitational attraction, and negative for an outward gravitational repulsion.

The Einstein field equations are given by [9]

$$m' = 4\pi r^2\rho, \tag{2}$$

$$\alpha' = \frac{m + 4\pi r^3 p_r}{r(r-2m)}, \tag{3}$$

$$p_r' = -\frac{(\rho + p_r)(m + 4\pi r^3 p_r)}{r(r-2m)} + \frac{2}{r}(p_t - p_r), \tag{4}$$

where $\rho(r)$ is the energy density, $p_r(r)$ is the radial pressure, and $p_t(r)$ is the tangential pressure orthogonal to p_r. Note that Eq. (4) corresponds to the anisotropic pressure Tolman-Oppenheimer-Volkoff equation.

An additional constraint is placed on the system of equations by considering the dark-energy equation of state $p_r(r) = \omega\rho(r)$ and taking into account Eqs. (2) and (3), we have the following relationship:

$$\alpha'(r) = \frac{m + \omega r m'}{r(r-2m)}. \tag{5}$$

There is, however, a subtle point that needs to be emphasized [5,6]. The notion of dark energy is that of a spatially homogeneous cosmic fluid. Nevertheless, it can be extended to inhomogeneous spherically symmetric spacetimes by regarding that the pressure in the equation of state $p = \omega\rho$ is a radial pressure, and that the transverse pressure may be obtained from Eq. (4). In addition to this, and as mentioned in the introduction, despite the fact that the dark-energy equation of state represents a spatially homogeneous cosmic fluid and is assumed not to cluster, inhomogeneities may arise due to gravitational instabilities. Thus, the dark-energy star geometries considered here may possibly originate from density fluctuations in the cosmological background, resulting in the nucleation through the respective density perturbations [11].

In Ref. [9], specific solutions were found by considering that the energy density is positive and finite at all points in the interior of the dark-energy star. In particular, several relativistic dark-energy stellar configurations were analyzed by imposing specific choices for the mass function $m(r)$, and through Eq. (5), $\alpha(r)$ was determined, consequently providing explicit expressions for the stress-energy tensor components. This interior solution was further matched to an exterior Schwarzschild vacuum solution given by

$$ds^2 = -\left(1-\frac{2M}{r}\right)dt^2 + \left(1-\frac{2M}{r}\right)^{-1}dr^2 + r^2(d\theta^2 + \sin^2\theta d\phi^2), \tag{6}$$

at a junction interface a. The Schwarzschild spacetime

possesses an event horizon at $r_b = 2M$, so that to avoid the latter, the junction radius lies outside $2M$, i.e., $a > 2M$.

The surface stresses on the thin shell are given by

$$\sigma = -\frac{1}{4\pi a}\left(\sqrt{1-\frac{2M}{a}+\dot{a}^2}-\sqrt{1-\frac{2m}{a}+\dot{a}^2}\right), \quad (7)$$

$$\mathcal{P} = \frac{1}{8\pi a}\left(\frac{1-\frac{M}{a}+\dot{a}^2+a\ddot{a}}{\sqrt{1-\frac{2M}{a}+\dot{a}^2}} - \frac{1+\omega m'-\frac{m}{a}+\dot{a}^2+a\ddot{a}+\frac{\dot{a}^2 m'(1+\omega)}{1-2m/a}}{\sqrt{1-\frac{2m}{a}+\dot{a}^2}}\right), \quad (8)$$

where σ and $\mathcal{P}$ are the surface energy density and the tangential surface pressure [9,32,33], respectively. The overdot denotes a derivative with respect to τ, which is the proper time on the junction interface, and the prime here denotes a derivative with respect to the junction surface radius a.

The dynamical stability of the transition layer a of these dark-energy stars to linearized spherically symmetric radial perturbations about static equilibrium solutions was also explored. It was found that large stability regions exist that are sufficiently close to where the event horizon is expected to form, so that it would be difficult to distinguish the exterior geometry of the dark-energy stars, analyzed in [9], from an astrophysical black hole.

B. Time-dependent spacetime

In this section, we generalize the above static dark-energy star models to time-dependent geometries. This is mainly motivated by the fact that recent fits to supernovae, cosmic microwave background radiation, and weak gravitational lensing data probably favor an evolving equation of state, with the dark-energy parameter crossing the phantom divide $\omega = -1$ [7].

In the following, we consider a time-dependent and spherically symmetric metric given by

$$ds^2 = -e^{2\alpha(r,t)}dt^2 + e^{2\beta(r,t)}dr^2 + r^2(d\theta^2+\sin^2\theta d\phi^2). \quad (9)$$

Note that one may also define the function $\beta(r,t)$ as

$$\beta(r,t) = \frac{1}{2}\ln\left[1-\frac{2m(r,t)}{r}\right], \quad (10)$$

where the "mass function" $m(r,t)$ is now time dependent.

The Einstein field equation provides the following nonzero components:

$$\rho(r,t) = \frac{e^{-2\beta}}{8\pi r^2}(2\beta' r + e^{2\beta} - 1), \quad (11)$$

$$p_r(r,t) = \frac{e^{-2\beta}}{8\pi r^2}(2\alpha' r - e^{2\beta} + 1), \quad (12)$$

$$f(r,t) = \frac{\dot{\beta}e^{-(\alpha+\beta)}}{4\pi r}, \quad (13)$$

$$p_t(r,t) = \frac{1}{8\pi}\left\{e^{-2\beta}\left[\alpha'' + \alpha'^2 - \alpha'\beta' + \frac{1}{r}(\alpha'-\beta')\right] + e^{-2\alpha}(\dot{\alpha}\dot{\beta} - \ddot{\beta} - \dot{\beta}^2)\right\}, \quad (14)$$

where the prime denotes a partial derivative with respect to the radial coordinate r, and the overdot a partial derivative with respect to the time coordinate t. Note the presence of an energy flux term in the radial direction, $T^t{}_r = \pm f(r,t)$, which depends on $\dot{\beta}$.

An important issue in the time-dependent dark-energy stars with the parameter crossing the phantom divide are the energy conditions, in particular, the NEC. The NEC is defined as $T_{\mu\nu}k^\mu k^\nu \geq 0$, where k^μ is any null vector, and consequently provides $\rho + p_r \pm 2f \geq 0$. The latter definition, taking into account the field Eqs. (11)–(13), is given by

$$\rho + p_r \pm 2f = \frac{1}{4\pi r}[e^{-2\beta}(\alpha'+\beta') \pm 2\dot{\beta}e^{-(\alpha+\beta)}] \geq 0. \quad (15)$$

In this context, one may consider a generalization of the equation of state $p_r = \omega\rho$, given by

$$p_r(r,t) = \omega(r,t)[\rho(r,t) \pm 2f(r,t)], \quad (16)$$

or

$$p_r(r,t) \mp 2f(r,t) = \omega(r,t)\rho(r,t), \quad (17)$$

where $f(r,t) = \mp T^t{}_r$ is the energy flux term, as noted above. However, one can come up with an interesting class of solutions considering the following equation of state:

$$p_r(r,t) = \omega(r,t)\rho(r,t). \quad (18)$$

Throughout this work, we essentially use the equation of state given by Eq. (18).

Taking into account the field Eqs. (11) and (12), then Eq. (18) provides the following relationship:

$$\omega(r,t)\beta'(r,t) = \alpha'(r,t) + \frac{1}{2r}[1+\omega(r,t)][1-e^{2\beta(r,t)}]. \quad (19)$$

A similar analysis was carried out in Ref. [34], in the context of time-dependent wormholes.

Equation (19) may be formally solved in terms of $\alpha(r,t)$, and provides the following general solution:

$$\alpha(r,t) = \int \frac{1}{\bar{r}}\left\{\omega(\bar{r},t)\beta'(\bar{r},t)\bar{r} - \frac{1}{2}[1+\omega(\bar{r},t)][1-e^{2\beta(\bar{r},t)}]\right\}d\bar{r}. \quad (20)$$

Thus, in principle, if $\omega(r,t)$ and $\beta(r,t)$ are known, then $\alpha(r,t)$ may be obtained from Eq. (20).

As an alternative, Eq. (19) can be formally integrated for $\beta(r, t)$ to yield the general solution

$$\beta(r, t) = -\frac{1}{2}\ln\left[-2F(t) + \int \frac{e^{\Gamma(\bar{r},t)}(1 + \omega(\bar{r}, t))}{\omega(\bar{r}, t)\bar{r}} d\bar{r}\right] + \frac{1}{2}\Gamma(r, t), \quad (21)$$

where $F(t)$ is an integration function, and the factor $\Gamma(r, t)$ is defined as

$$\Gamma(r, t) = \int\left[\frac{2\bar{r}\alpha'(\bar{r}, t) + \bar{r} + 1}{\bar{r}\omega(\bar{r}, t)}\right] d\bar{r}. \quad (22)$$

A particularly simple and interesting toy model is the specific case of a purely time-dependent parameter $\omega = \omega(t)$, so that the general solution (21) takes the form

$$\beta(r, t) = -\frac{1}{2}\left\{\frac{2\alpha(r, t)}{\omega(t)} - \ln\left[r^{-(1+\omega(t)/\omega(t))}(-2F(t) + \frac{1 + \omega(t)}{\omega(t)}\int e^{2\alpha(\bar{r},t)/\omega(t)}\bar{r}^{1/\omega(t)} d\bar{r}\right)\right]\right\}. \quad (23)$$

In the next section, we analyze specific solutions, namely, that of a constant energy density, the Tolman-Matese-Whitman mass function, which were extensively explored in Ref. [9], and a collapsing model with a nonzero energy flux term.

III. SPECIFIC TIME-DEPENDENT DARK-ENERGY STAR SOLUTIONS

A. Constant energy density

Consider the specific case of a constant energy density, $\rho(r, t) = \rho_0$, so that Eq. (11) provides the solution

$$\beta(r, t) = -\frac{1}{2}\ln\left[1 - Ar^2 + \frac{F_1(t)}{r}\right], \quad (24)$$

with $A = 8\pi\rho_0/3$, and $F_1(t)$ is a function of integration.

Substituting into Eq. (20), one arrives at

$$\alpha(r, t) = \int \frac{3A\omega(r, t)r^3 + Ar^3 - 3F_1(t)}{2r[3r - Ar^3 + 3F_1(t)]} + F_2(t), \quad (25)$$

where $F_2(t)$ is another function of integration. One may further simplify the analysis by considering that $F_1(t) = 0$, which is physically justified by the imposition of a finite mass function at the origin $r = 0$ for all values of the time coordinate t. Note that considering $F_1(t) = 0$ implies that the mass function is not time dependent, and the flux term $f(r, t)$ is zero, as $\dot{\beta} = 0$.

For instance, consider the specific example of a separation of variables of the parameter $\omega(r, t)$ given by

$$\omega(r, t) = \omega_1(t)\omega_2(r). \quad (26)$$

Choosing the following functions,

$$\omega_1(t) = \omega_0 + \bar{\omega}_0 \tanh[\sigma(t - t_0)], \quad (27)$$

$$\omega_2(r) = -\frac{\lambda^2}{1 + (r/R)^2}, \quad (28)$$

where ω_0, $\bar{\omega}_0$, σ, t_0, λ^2, and R are constants. The factor $1/\sigma$ may be interpreted as the "relaxation time," describing the width of the time dependence.

See Fig. 1 for a qualitative description of $\omega(r, t)$ given by Eqs. (26)–(28). The left plot represents the behavior of $\omega = \omega(0, t)$ at the center $r = 0$. We have considered the following values: $R = 1$, $\delta = 1$, $\omega_0 = 3/4$, $\bar{\omega}_0 = 2/3$ and $t_0 = 8$.

Substituting the functions (26)–(28) into Eq. (25), yields the following solution:

$$\alpha(r, t) = \frac{1}{4}\ln\left\{\frac{(1 - Ar^2)^{\bar{A}\omega_1(t)-1}}{[1 + (r/R)^2]^{\bar{A}\omega_1(t)}}\right\} + F_2(t), \quad (29)$$

where, for notational simplicity, the constant $\bar{A}$ is defined as

$$\bar{A} = \frac{3AR^2\lambda^2}{R^2A + 1}. \quad (30)$$

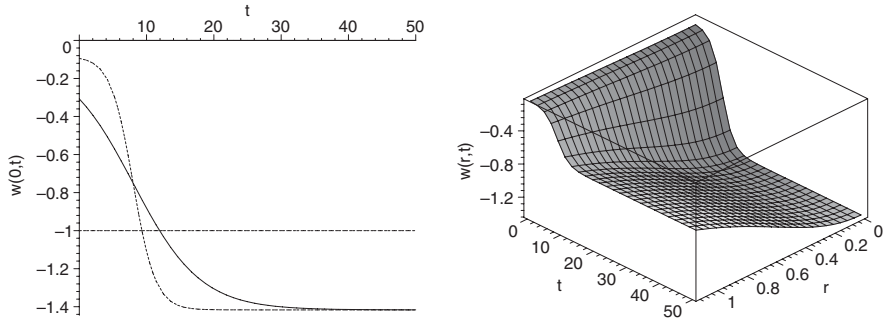

FIG. 1. Left plot: For this case, we considered the behavior of $\omega = \omega(0, t)$ at the center $r = 0$; for the dashed curve we have $\sigma = 0.3$ and for the solid curve $\sigma = 0.1$. Right plot: For this case, we considered the $\omega = \omega(t, r)$ dependence with $\sigma = 0.3$. For both cases, we have assumed the following numerical values: $R = 1$, $\delta = 1$, $\omega_0 = 3/4$, $\bar{\omega}_0 = 2/3$, and $t_0 = 8$.

The function $F_2(t)$ can be absorbed through a redefinition of the time coordinate as before, so that without a significant loss of generality one may impose the condition $F_2(t) = 0$.

The pressure profile is given by

$$p_r = -\frac{3\lambda^2 R^2 A\omega_1(t)}{8\pi(R^2 + r^2)}, \tag{31}$$

$$p_t = \frac{3A}{32\pi}\frac{R^2Ar^2(R^2 + 2r^2) + Ar^6 + \omega_1(t)\lambda^2R^2[3Ar^2\omega_1(t)\lambda^2R^2 - 4(Ar^4 + R^2)]}{(1 - Ar^2)(R^2 + r^2)^2}, \tag{32}$$

with $p_r = p_t$ at the center $r = 0$.

The analysis simplifies by considering a purely time-dependent parameter, i.e., $\omega = \omega(t)$. Thus, Eq. (25) takes the form

$$\alpha(r, t) = -\frac{1}{4}[1 + 3\omega(t)]\ln(1 - Ar^2) + F_2(t). \tag{33}$$

The pressure profile is given by the following relationships:

$$p_r = \frac{3A\omega(t)}{8\pi}, \qquad p_t = \frac{3A[4\omega(t) + Ar^2 + 3Ar^2\omega^2(t)]}{32\pi(1 - Ar^2)}. \tag{34}$$

Note that $p_r = p_t$ at the center $r = 0$ as expected.

B. Tolman-Matese-Whitman mass function

An interesting example is the Tolman-Matese-Whitman mass function considered in Ref. [9]. As in the example outlined above, we impose that $\dot{\beta} = 0$, so that the flux term $f(r, t)$ is zero. Thus, consider the following choice for the time-independent mass function, given by

$$\beta(r, t) = \beta(r) = \frac{1}{2}\ln\left(\frac{1 + 2b_0r^2}{1 + b_0r^2}\right), \tag{35}$$

where b_0 is a non-negative constant [9]. The latter may be determined from the regularity conditions and the finite character of the energy density at the origin $r = 0$, and is given by $b_0 = 8\pi\rho_c/3$, where ρ_c is the energy density at $r = 0$.

Now, consider the radial and temporal dependent case of $\omega = \omega(r, t)$ given by the functions (26)–(28). Substituting these functions and Eq. (35) into Eq. (20), yields the following solution:

$$\alpha(r, t) = \frac{1}{2}\ln\left\{(1 + b_0r^2)^{\Sigma(t)}(1 + 2b_0r^2)^{\Upsilon(t)}\left[1 + \left(\frac{r}{R}\right)^2\right]^{\Xi(t)}\right\} + F_2(t), \tag{36}$$

where the $F_2(t)$ is a function of integration that may be reabsorbed in a redefinition of the time coordinate, so that without a loss of generality we impose $F_2(t) = 0$, as before. For notational simplicity, we have considered the following definitions:

$$\Sigma(t) = \frac{1 + b_0R^2(2b_0R^2 - 3) - b_0\lambda^2R^2\omega_1(t)(1 - 2b_0R^2)}{2(1 - 2R^2b_0)(1 - R^2b_0)}, \tag{37}$$

$$\Upsilon(t) = \frac{2b_0\lambda^2R^2}{1 - 2R^2b_0}, \tag{38}$$

$$\Xi(t) = \frac{b_0\lambda^2R^2\omega_1(t)(2b_0R^2 - 3)}{2(1 - 2R^2b_0)(1 - R^2b_0)}, \tag{39}$$

respectively.

The stress-energy tensor components are given by

$$\rho(r) = \frac{b_0(3 + 2b_0r^2)}{8\pi(1 + 2b_0r^2)^2}, \tag{40}$$

$$p_r(r, t) = -\frac{b_0R^2\lambda^2(3 + 2b_0r^2)\omega_1(t)}{8\pi(R^2 + r^2)(1 + 2b_0r^2)^2}, \tag{41}$$

$$\begin{aligned} p_t(r, t) = b_0[&4R^4b_0^3r^6(1 - \omega_1(t)\lambda^2)^2 + 8R^2b_0^3r^8(1 + \omega_1(t)\lambda^2) + 4R^4b_0^2r^4(2 - 3\omega_1(t)\lambda^2 + 3\omega_1(t)\lambda^4) \\ &+ 4R^2b_0^2r^6(4 + 9\omega_1(t)\lambda^2) + R^4b_0r^2(3 - 16\omega_1(t)\lambda^2 + 9\omega_1^2(t)\lambda^4) + 2R^2b_0r^4(3 + 14\omega_1(t)\lambda^2) \\ &+ b_0r^6(3 + 8b_0r^2 + 4b_0^2r^4) - 12\omega_1(t)R^4\lambda^2]/[32\pi(1 + b_0r^2)(1 + 2b_0r^2)^3(R^2 + r^2)^2]. \end{aligned} \tag{42}$$

Note that $p_r = p_t$ at the center $r = 0$.

For simplicity, considering a purely time-dependent parameter $\omega = \omega(t)$, and substituting (35) into Eq. (20), provides the following solution:

$$\alpha(r, t) = \frac{1}{2}\ln[(1 + b_0r^2)^{1-\omega(t)/2}(1 + 2b_0r^2)^{\omega(t)}] + F(t), \tag{43}$$

where the $F(t)$ is a function of integration which, as before, may be absorbed into a redefinition of the time coordinate, so

that one may consider $F(t) = 0$ without a significant loss of generality.

The stress-energy tensor components are given by

$$p_r = \omega(t)\rho = \frac{b_0(3 + 2b_0r^2)\omega(t)}{8\pi(1 + 2b_0r^2)^2}, \tag{44}$$

$$p_t = \frac{b_0\{4b_0^2r^4(1 + \omega)[3 + b_0r^2(1 + \omega)] + b_0r^2[3 + \omega(9\omega + 16)] + 8b_0^2r^4 + 12\omega\}}{32\pi(1 + b_0r^2)(1 + 2b_0r^2)^3}, \tag{45}$$

with $p_r = p_t$ at the center, $r = 0$.

C. A class of models with a nonzero flux term

In this section, we construct a set of models with a nonzero energy flux term, where at early times possesses a small inhomogeneity in the region near $r = 0$, which grows due to gravitational collapse. For the specific case considered in this section, we assume for simplicity that the parameter, which eventually crosses the phantom divide in the central region, is purely time dependent, i.e., $\omega = \omega(t)$, and is governed by an equation of state of the form

$$p_r(r, t) = \omega(t)\rho(r, t), \tag{46}$$

and that the system tends to isotropy for large r.

For the energy density, we generalize the Mbonye-Kazanas density profile [35] (also utilized by Dymnikova [36]) to a reasonable time-dependent model given by

$$\rho(r, t) = \rho_0 a(t) e^{-(r/r_0)^n}, \tag{47}$$

where ρ_0, r_0, and n are appropriately chosen constants. Here, the time-dependent function $a(t)$ is chosen so that the collapse will asymptote at late times, forming a static star. Note for the sake of clarity that the time-dependent function $a(t)$ should not be confused with the junction interface radius introduced in Eqs. (7) and (8). This profile has been extremely useful in the investigations of nonsingular black holes (i.e., horizons not shielding a singularity) [35], including de Sitter core black holes [36] and, more recently, as a model for gravastars [15] (supplemented with an appropriate equation of state).

The equation of state (46) then yields

$$p_r(r, t) = \omega(t)\rho_0 a(t) e^{-(r/r_0)^n}. \tag{48}$$

At this stage, it is useful to write the solution to the field equations as follows [37]:

$$e^{-2\beta(r,t)} = 1 - \frac{8\pi}{r}\left[b^2(t) + \int_{0_+}^{r} \rho(\bar{r}, t)\bar{r}^2 d\bar{r}\right], \tag{49a}$$

$$e^{2\alpha(r,t)} = e^{-2\beta(r,t)}\left\{\exp\left[h(t) + 8\pi\int_{0_+}^{r}[p_r(\bar{r}, t) + \rho(\bar{r}, t)]e^{2\beta(\bar{r},t)}\bar{r}d\bar{r}\right]\right\}, \tag{49b}$$

$$f(r, t) = -\frac{1}{r^2}\left[2b(t)\dot{b}(t) + \int_{0_+}^{r} \dot{\rho}(\bar{r}, t)\bar{r}^2 d\bar{r}\right]e^{2[\beta(r,t)-\alpha(r,t)]}, \tag{49c}$$

$$p_t(r, t) = \frac{r}{2}(p_r' + \dot{f}) + \left(1 + \frac{r}{2}\alpha'\right)p_r + \frac{r}{2}(\dot{\alpha} + \dot{\beta})f + \frac{r}{2}\alpha'\rho, \tag{49d}$$

respectively, where the explicit coordinate dependence has been dropped in Eq. (49d), and as before, the prime denotes a partial derivative with respect to the radial coordinate r, and the overdot a partial derivative with respect to the time coordinate t. The functions $b(t)$ and $h(t)$ are two arbitrary functions of integration. For a star, $b(t)$ is set to zero to avoid a singularity at the center. However, at late time this function need not vanish as it is useful for the wormhole configuration. Note that with the prescription of the energy density and radial pressure, the entire system of equations may, in principle, be solved for the unknowns. We exploit this fact here. To ensure that the star crosses the phantom divide and yet does not collapse for infinite time, the following prescriptions are made:

$$\begin{aligned} a(t) &= a_0[(1 + \epsilon) - e^{-k_0 t}], \\ \omega(t) &= \omega_0 - \omega_1(1 - e^{-k_1 t}), \end{aligned} \tag{50}$$

where 0 and 1 subscripts denote constant quantities. We now have an infinite family of solutions with the desired physical properties. At this stage we should note that the generated spacetimes tend to Minkowski spacetime as $r \to \infty$. One would need to therefore cut off the solution at some $r = r_*$ and patch it to an appropriate dark-energy exterior. However, given how small the energy density and pressures of the currently accelerating Universe are (when compared with those of an average star), the asymptotic Minkowski approximation is probably a reasonable approximation.

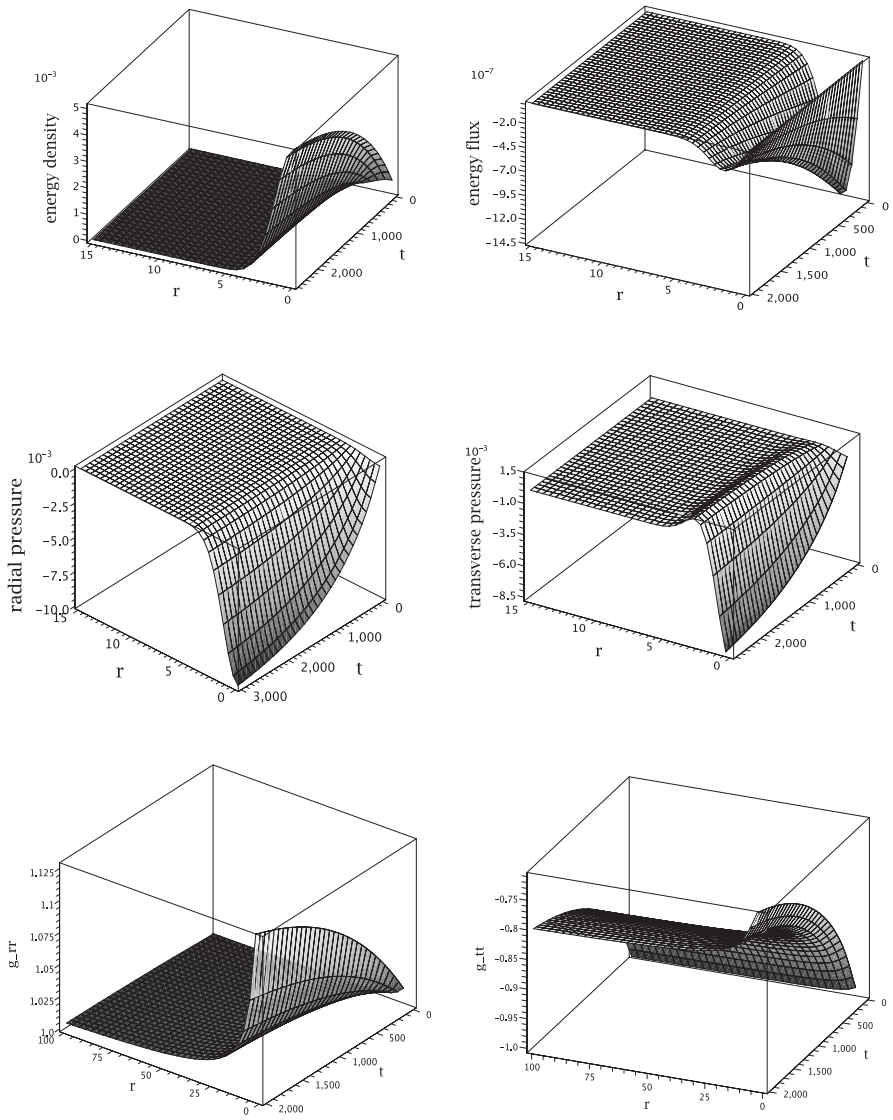

FIG. 2. Parameters for a sample stellar model presented in Sec. III C. Plotted on the vertical axes (from left to right, starting from the top) are $\rho(r, t)$, $T^t_r(r, t)$ $p_r(r, t)$, $p_t(r, t)$, and finally $e^{2\beta(r,t)}$ and $-e^{2\alpha(r,t)}$.

Surprisingly, for certain values of n, the Eqs. (49a)–(49d) may actually be integrated to yield an analytic result. The expressions are rather unwieldly however so instead we plot the various relevant parameters in Figs. 2 and 3. From the figures it can be noted that the initial inhomogeneity is very small, most pronounced near the center, and

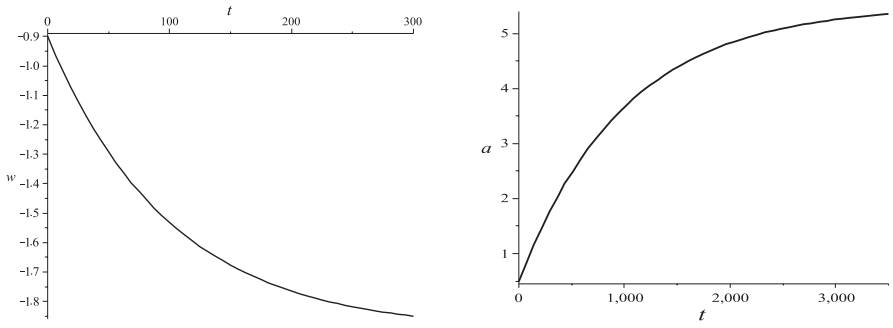

FIG. 3. The parameters $\omega(t)$ (left) and $a(t)$ (right) for a sample stellar model presented in Sec. III C. For this particular evolution, the following values were used: $\omega_0 = -0.9$, $k_1 = 0.01$, $a_0 = 5$, $\epsilon = 0.1$, $k_0 = 0.001$, $\omega_1 = 1$.

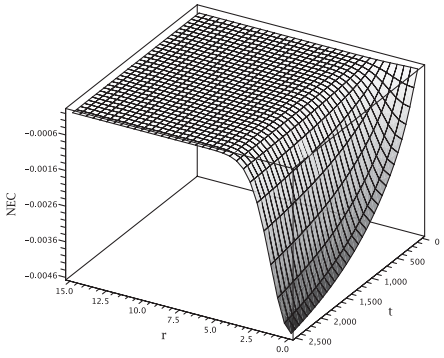

FIG. 4. The figure depicts the null energy condition NEC $= \rho + p_r + 2f$ for the specific model with a nonzero flux term considered in the text.

the spacetime almost flat everywhere. There is an inward flow of energy, due to the gravitational collapse as can be seen by the negative values of the energy flux plot. At late time, the magnitude of the energy flux decreases and asymptotes to zero, indicating the halt of the collapse. At some point during the collapse, the phantom divide is crossed and the conditions for possible wormhole formation are established. We show this in Fig. 4 where it may be seen that the NEC violation is most severe in the center.

IV. TOPOLOGY CHANGE: THE CASIMIR ENERGY APPROACH

Although (50) also allows for an *ordinary* (positive pressure) fluid at early times, all of the geometries considered in the previous sections were modeled so that the evolving parameter $\omega(r, t)|_{r=0}$ starts out in the range $-1 < \omega < -1/3$, then crosses the phantom divide, and finally ends up in the phantom regime $\omega = p_r/\rho < -1$. Once in the phantom regime, the negative radial pressure exceeds the energy density, which in principle may imply a topology change. It is still uncertain how to obtain this topology change, and if possible, is riddled with difficulties, such as the theoretical appearance of closed timelike curves. It is likely that crossing the phantom divide is accompanied by a large quantum fluctuation of the metric. Then a crucial question is [27] what happens when the metric fluctuations become large?

In some cases, we can create a one to one correspondence between topology and the asymptotic energy. In particular, we will consider the Arnowitt-Deser-Misner (ADM) energy [38] as a reference energy. The reason for such a choice is that $E_{\mathrm{ADM}} \geq 0$, and it is vanishing for flat space. Therefore, we can think about flat space as the unique reference space to compare a change in spacetime associated to the corresponding topology. A trivial example could be the comparison between flat space, where the topology is R^4 and the Schwarzschild space, with topology $R^2 \times S^2$: they are topologically distinct and possess a distinct ADM energy: $E_{\mathrm{flat}} = 0$ and $E_{\mathrm{Schwarzschild}} = M$. A topology transition from Schwarzschild to flat or vice versa, should be necessarily accompanied by a change in ADM energy. In the same manner, we can think that a transition from the dark star to the wormhole could be associated to a change in the asymptotic energy, measured by the ADM energy, namely, if a topology change appears, this could be reflected to a change in the ADM energy. The way to detect this is simply computed by

$$E^{\mathrm{DS}}_{\mathrm{ADM}} - E^{\mathrm{Wormhole}}_{\mathrm{ADM}} = (E^{\mathrm{DS}}_{\mathrm{ADM}} - E^{\mathrm{Flat}}_{\mathrm{ADM}}) - (E^{\mathrm{Wormhole}}_{\mathrm{ADM}} - E^{\mathrm{Flat}}_{\mathrm{ADM}})0. \quad (51)$$

For asymptotically flat spacetimes, the ADM energy is defined as

$$E_{\mathrm{ADM}} = \frac{1}{16\pi G}\int_S (D^i h_{ij} - D_j h) r^j, \quad (52)$$

where the indices i, j run over the three spatial dimensions and

$$h_{ij} = g_{ij} - \bar{g}_{ij}, \quad (53)$$

where $\bar{g}_{ij}$ is the background three-metric. D_j is the background covariant derivative and r^j is the unit normal to the large sphere S. However, Hawking and Horowitz [39] have shown that the definition (52) is equivalent to

$$E_{\mathrm{ADM}} = \frac{1}{8\pi G}\int_{S^\infty} d^2x\sqrt{\sigma}(k - k^0), \quad (54)$$

where σ is the determinant of the unit 2 sphere. k^0 represents the trace of the extrinsic curvature corresponding to embedding in the two-dimensional boundary $2S$ in three-dimensional Euclidean space at infinity. In an alternative to the ADM energy, we can use quasilocal energy to compute such a difference, which is defined by Eq. (54) but for a finite 2 sphere. The main reason to use such a definition is that we can extend the surface energy computation even to nonasymptoticaaly flat spaces. For this purpose, consider a manifold $\mathcal{M}$ composed by two wedges $\mathcal{M}_+$ and $\mathcal{M}_-$, located in the right and left sectors of a Kruskal diagram, respectively, and bounded by two three-dimensional disconnected timelike boundaries B_+ and B_- located in $\mathcal{M}_+$ and $\mathcal{M}_-$, respectively. The quasilocal energy E_{tot} of a spacelike hypersurface $\Sigma = \Sigma_+ \cup \Sigma_-$ bounded by two spacelike boundaries S_+ and S_- located in $\mathcal{M}_+$ and $\mathcal{M}_-$, respectively, is given by [40–42]

$$E_{\mathrm{tot}} = E_+ - E_-.$$

More specifically, E_{tot} is defined as the value of the Hamiltonian that generates unit time translations orthogonal to the two-dimensional boundaries [40–42]. E_+ and E_- are defined as

$$\begin{cases} E_+ = \frac{1}{8\pi G}\int_{S_+} d^2x\sqrt{\sigma}(k - k^0) \\ E_- = -\frac{1}{8\pi G}\int_{S_-} d^2x\sqrt{\sigma}(k - k^0) \end{cases}, \quad (55)$$

respectively. The trace of the second fundamental form k is defined as

$$k = -\frac{1}{\sqrt{h}}(\sqrt{h}n^{\mu})_{,\mu}, \tag{56}$$

where n^{μ} is the normal to the boundaries, and h is the determinant of the metric of Σ. As an example, consider the static Einstein-Rosen bridge, with the metric given by

$$ds^2 = -N^2dt^2 + g_{yy}dy^2 + r^2(y)d\Omega^2, \tag{57}$$

where the lapse function N, g_{yy}, and r are functions of the radial coordinate y continuously defined on $\mathcal{M}$, with $dy = dr/\sqrt{1-2MG/r}$. The boundaries S_+ and S_- are located at coordinate values $y = y_+$ and $y = y_-$, respectively, and the lapse function is given by $|N| = 1$ at both S_+ and S_-. In this case, $n^{\mu} = (g^{yy})^{1/2}\delta^{\mu}_{y}$. Since this normal is defined continuously along Σ, the value of k depends on the function $r_{,y}$, which is positive for B_+ and negative for B_-. See Fig. 5 for a Penrose-Carter diagram illustrating the boundary locations in a Schwarzschild metric.

From Eqs. (56) and (57), we obtain at either boundary that

$$k = -\frac{2r_{,y}}{r}, \tag{58}$$

where we have assumed that the function $r_{,y}$ is positive for S_+ and negative for S_-. The trace associated with the subtraction term is taken to be $k^0 = -2/r$ for B_+ and $k^0 = 2/r$ for B_-. As an illustration, consider the case when the boundary B_+ is located at right-hand infinity ($y_+ = +\infty$) and the boundary B_- is located at y_-, then

$$E_{\rm tot} = M - r\left[1 - \left(1 - \frac{2MG}{r}\right)^{1/2}\right]. \tag{59}$$

It is easy to see that E_+ and E_- tend individually to the ADM mass M when the boundaries ${}^3B_+$ and ${}^3B_-$ tend, respectively, to right and left spatial infinity. It should be noted that the total energy is zero for boundary conditions symmetric with respect to the bifurcation surface, i.e.,

$$E = E_+ - E_- = M + (-M) = 0. \tag{60}$$

Consider now the dark-energy star of metric (1) and a wormhole defined by the *shape function* $b(r)$, with the following difference:

$$\begin{cases} \text{Dark energy star (DS)}, & m(r) \text{ with } r \in [0, +\infty) \\ \text{Wormhole } (W), & b(r) \text{ with } r \in [r_0, +\infty). \end{cases} \tag{61}$$

Consider also the relation (51). Thus, by repeating the computation leading to Eqs. (59) and (60) in the case of interest, we get

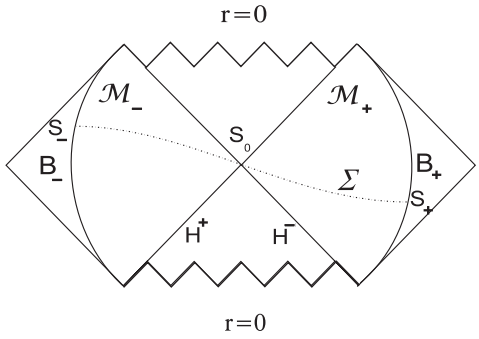

FIG. 5. A Penrose-Carter diagram illustrating the boundary location in a Schwarzschild metric. $\mathcal{M}_+$ and $\mathcal{M}_-$ are the two wedges, located in the right and left sectors of a Kruskal diagram, respectively, and bounded by two boundaries B_+ and B_- located in $\mathcal{M}_+$ and $\mathcal{M}_-$, respectively. $\Sigma = \Sigma_+ \cup \Sigma_-$ is a spacelike hypersurface. H_+ and H_- are the future and past horizon, respectively. S_0 ($S_0 = H_+ \cap H_-$) is the bifurcation surface (wormhole throat), and S_+ and S_- are the two-dimensional boundaries of Σ_+ and Σ_-, respectively.

$$\begin{aligned} k^W - k^{\rm DS} &= (k-k^0)^W - (k-k^0)^{\rm DS} \\ &= \frac{-2}{r}(r_{,y}-1)^W - \frac{-2}{r}(r_{,y}-1)^{\rm DS} \\ &= \frac{-2}{r}\left[\sqrt{1-\frac{b(r)}{r}} - \sqrt{1-\frac{2m(r)}{r}}\right], \end{aligned} \tag{62}$$

where we are looking at the positive wedge $\mathcal{M}_+$ only. For large boundaries $R \gg r_0$ and expanding around the throat, one obtains

$$\begin{aligned} k^W - k^{\rm DS} &= \frac{-2}{r}\left[\sqrt{1-\frac{b(r_0)+b'(r_0)(r-r_0)+\ldots}{r}} \right. \\ &\quad \left. - \sqrt{1-\frac{2m(r)}{r}}\right], \end{aligned} \tag{63}$$

$$\begin{aligned} &\simeq \frac{-2}{R}\left[\left(1-\frac{b(r_0)+b'(r_0)(r-r_0)+\ldots}{2R}\right)\right. \\ &\quad \left. - \left(1-\frac{m(R)}{R}\right)\right] \\ &= \frac{1}{R^2}[r_0 + b'(r_0)(r-r_0) - 2m(R)], \end{aligned} \tag{64}$$

where we have used the wormhole condition at the throat $b(r_0) = r_0$. If $b'(r_0) = 0$ and $m(R)$ are negligible, then we recover the ADM mass. Indeed, by integrating on the boundary ${}^2S_+$, we obtain

$$E_+ = \frac{r_0}{2G} = M. \tag{65}$$

If $b'(r_0) \neq 0$ and $m(R)$ is not vanishing, then the evaluation of the energy depends on a case to case scenario. The same

discussion can be applied on the negative wedge. As shown in Eq. (60), if we choose boundaries symmetric with respect to the bifurcation surface, here represented by the throat r_0, we have a total zero ADM-like energy. The physical situation looks like a familiar QED physical process $\gamma \rightarrow e^+e^-$: the electric charge is conserved. In our case, the charge is the asymptotic energy. Since there is no reason to have an asymmetry in boundaries in the absence of external forces, we have to conclude that the classical term is not able to predict the appearance of a wormhole or the permanence of a dark star. We are forced to compute quantum effects. The implicit subtraction procedure of Eq. (55) can be extended in such a way that we can include quantum effects: this is the Casimir energy or in other terms, the vacuum energy. One can in general formally define the Casimir energy as follows:

$$E_{\text{Casimir}}[\partial\mathcal{M}] = E_0[\partial\mathcal{M}] - E_0[0], \tag{66}$$

where E_0 is the zero-point energy, $\partial\mathcal{M}$ is a boundary and $E_0[0]$ represents the zero-point energy without a boundary. For zero temperature, the idea underlying the Casimir effect is to compare vacuum energies in two physical distinct configurations. The extension to quantum effects is straightforward:

$$E_{\text{Casimir}}[\partial\mathcal{M}] = (E_0[\partial\mathcal{M}] - E_0[0])_{\text{classical}} + (E_0[\partial\mathcal{M}] - E_0[0])_{\text{1-loop}} + \ldots. \tag{67}$$

In our picture, the classical part represented by the ADM-like energy is vanishing, because of the symmetry of boundary conditions. This means that

$$E_{\text{Casimir}}[\partial\mathcal{M}] = (E_0[\partial\mathcal{M}] - E_0[0])_{\text{1-loop}} + \ldots., \tag{68}$$

namely, E_{Casimir} is purely quantum. Thus, the Casimir energy can be regarded as a measure of the topology change. With this, we mean that, if E_{Casimir} is positive, then the topology change will be suppressed, while if it is negative, it will be favored. It is important to remark that in most physical situations, the Casimir energy is negative. Consider now the one loop term. We will evaluate it following the scheme of Eq. (62). Thus,

$$(E_0^W[\partial\mathcal{M}] - E_0^{\text{DS}}[\partial\mathcal{M}])_{\text{1-loop}} = (E_0^W[\partial\mathcal{M}] - E_0[0])_{\text{1-loop}} + (E_0[0] - E_0^{\text{DS}}[\partial\mathcal{M}])_{\text{1-loop}}. \tag{69}$$

The procedure followed to evaluate Eq. (69) relies heavily on the formalism outlined in Refs. [43,44]. The computation was realized through a variational approach with Gaussian trial wave functionals. A zeta function regularization is used to deal with the divergences, and a renormalization procedure is introduced, where the finite one loop is considered as a self-consistent source for traversable wormholes. Rather than reproduce the formalism, we shall refer the reader to Refs. [43,44] for details, when necessary. We can write,

$$\begin{aligned}(E_0^W[\partial\mathcal{M}] - E_0^{\text{DS}}[\partial\mathcal{M}])_{\text{1-loop}} &= \frac{1}{64\pi^2}\Bigg\{\Bigg[(m_L^2(r) + m_{1,S}^2(r))^2 \ln\Bigg(\frac{m_L^2(r) + m_{1,S}^2(r)}{4\mu_0^2}\sqrt{e}\Bigg) \\ &\quad + (m_L^2(r) + m_{2,S}^2(r))^2 \ln\Bigg(\frac{m_L^2(r) + m_{2,S}^2(r)}{4\mu_0^2}\sqrt{e}\Bigg)\Bigg]_W \\ &\quad - \Bigg[(m_L^2(r) + m_{1,S}^2(r))^2 \ln\Bigg(\frac{m_L^2(r) + m_{1,S}^2(r)}{4\mu_0^2}\sqrt{e}\Bigg) \\ &\quad + (m_L^2(r) + m_{2,S}^2(r))^2 \ln\Bigg(\frac{m_L^2(r) + m_{2,S}^2(r)}{4\mu_0^2}\sqrt{e}\Bigg)\Bigg]_{\text{DS}}\Bigg\},\end{aligned} \tag{70}$$

where we have defined two r-dependent effective masses $m_1^2(r)$ and $m_2^2(r)$, which can be cast in the following form:

$$\begin{cases} m_1^2(r) = m_L^2(r) + m_{1,S}^2(r) \\ m_2^2(r) = m_L^2(r) + m_{2,S}^2(r) \end{cases}, \tag{71}$$

where

$$m_L^2(r) = \frac{6}{r^2}\Bigg(1 - \frac{b(r)}{r}\Bigg), \tag{72}$$

and

$$\begin{cases} m_{1,S}^2(r) = [\frac{3}{2r^2}b'(r) - \frac{3}{2r^3}b(r)] \\ m_{2,S}^2(r) = [\frac{1}{2r^2}b'(r) + \frac{3}{2r^3}b(r)] \end{cases}, \tag{73}$$

respectively. We refer the reader to Refs. [43,44] for the deduction of these expressions in the Schwarzschild case. The zeta function regularization method has been used to determine the energy densities, ρ_i. It is interesting to note that this method is identical to the subtraction procedure of the Casimir energy computation, where the zero-point energy in different backgrounds with the same asymptotic properties is involved. In this context, the additional mass parameter μ has been introduced to restore the correct dimension for the regularized quantities. Note that this arbitrary mass scale appears in any regularization scheme. Of course $b(r) = 2m(r)$, then we can use only one function recalling the different boundary conditions they must satisfy. Generally speaking, we can adopt the condition $m(0) = 0$ for the dark-energy star and $b(r_0) = r_0$ for the wormhole. Thus, the leading part related to the dark-energy star close to $r = 0$, simply becomes

$$-(E_0[0] - E_0^{\text{DS}}[\partial\mathcal{M}])_{\text{1-loop}} \simeq \Bigg[-\frac{3}{16\pi^2 r^4}\ln\Bigg(\frac{6}{4r^2\mu_0^2}\sqrt{e}\Bigg)\Bigg]_{\text{DS}}.$$

On the other hand, for the wormhole we get at the throat [45]

$$(E_0^W[\partial\mathcal{M}] - E_0[0])_{1\text{-loop}} = \frac{1}{64\pi^2}\left[\frac{9}{4r_0^4}(b'(r_0)-1)^2 \ln\left(\left|\frac{b'(r_0)-1}{8r_0^2\mu_0^2}\sqrt{e}\right|\right) + \frac{1}{4r_0^4}(b'(r_0)+3)^2 \ln\left(\frac{b'(r_0)+3}{8r_0^2\mu_0^2}\sqrt{e}\right)\right]_W. \quad (74)$$

To have an easy comparison with the dark-energy star, we make a specific choice for the wormhole shape function. We assume that

$$b(r) = \frac{r_0^2}{r}, \quad (75)$$

then we obtain

$$(E_0^W[\partial\mathcal{M}] - E_0^{\mathrm{DS}}[\partial\mathcal{M}])_{1\text{-loop}} \simeq \frac{1}{64\pi^2}\left\{\frac{10}{r_0^4}\ln\left(\frac{\sqrt{e}}{4r_0^2\mu_0^2}\right) - \left[\frac{12}{r^4}\ln\left(\frac{6\sqrt{e}}{4r^2\mu_0^2}\right)\right]\right\}. \quad (76)$$

Moreover, we evaluate the dark-energy star term close to r_0 to get

$$(E_0^W[\partial\mathcal{M}] - E_0^{\mathrm{DS}}[\partial\mathcal{M}])_{1\text{-loop}} \simeq \frac{1}{32\pi^2 r_0^4}\left\{5\ln\left(\frac{\sqrt{e}}{4r_0^2\mu_0^2}\right) - \left[6\ln\left(\frac{6\sqrt{e}}{4r_0^2\mu_0^2}\right)\right]\right\}. \quad (77)$$

If we choose

$$\mu_0 \leq \frac{108\sqrt[4]{e}}{r_0} \Rightarrow (E_0^W[\partial\mathcal{M}] - E_0^{\mathrm{DS}}[\partial\mathcal{M}])_{1\text{-loop}} \leq 0. \quad (78)$$

It is important to remark that the result of inequality (78) is valid only for the class of traversable wormholes expressed by the shape function (75). To discuss the appearance of different class of traversable wormholes, we need to use expression (74) inside inequality (78), and it is quite evident that this strongly depends on the form of the shape function as it should be. It is interesting to note that once this has been created, there is a probability that it will be self-sustained [18], at least for an inhomogeneous ω parameter, like in our case. This means that quantum fluctuations related to the Casimir energy play a fundamental part not only for the topology change but even for the traversable wormhole persistence.

V. SUMMARY AND DISCUSSION

In this work, we have considered time-dependent dark-energy star models, with an evolving parameter ω crossing the phantom divide $\omega = -1$. In particular, we briefly reviewed static and spherically symmetric dark-energy stars, and further analyzed general solutions of time-dependent spacetimes in detail. Specific time-dependent solutions were extensively explored, in particular, the specific cases of a constant energy density, the Tolman-Matese-Whitman mass function solution, and a class of models with a nonzero energy flux term, which form from gravitational collapse. Once the parameter ω evolves into the phantom regime, the null energy condition is violated, which physically implies that the negative radial pressure exceeds the energy density. Therefore, an enormous negative pressure at the center may, in principle, imply a topology change, consequently opening up a tunnel and converting the dark-energy star into a wormhole. The theoretical difficulties and criteria for this topology change were discussed in detail, where, in particular, we considered a Casimir energy approach involving quasilocal energy difference calculations that may reflect or measure the occurrence of a topology change. Once the topology change has occurred, it is possible that the resulting wormhole structures, supported by phantom energy, be self-sustained. As mentioned in the introduction, recent fits to observational data probably favor an evolving equation of state, with the dark-energy parameter crossing the phantom divide $\omega = -1$ [7]. However, in a cosmological setting the transition into the phantom regime is physically implausible for a single scalar field [7], so that a possible approach would be to consider a mixture of interacting non-ideal fluids. One may consider that the time-dependent dark-energy star model outlined in this work, is a simplification of this possible approach. In fact, recently, static models with two interacting phantom and ghost scalar fields were considered, and it was shown that regular solutions exist [28]. It would be interesting to generalize the latter study to time-dependent solutions, extending the analysis considered in this work.

It is interesting to note that the topology change at the center should influence the surface stresses at the thin shell, as there is a redistribution of the stress-energy tensor components of the interior solution during the change in topology. That this is so may be verified through the conservation identity given by $S^i_{j|i} = [T_{\mu\nu}e^\mu_{(j)}n^\nu]^+_-$, where $[X]^+_-$ denotes the discontinuity across the surface interface Σ, i.e., $[X]^+_- = X^+|_\Sigma - X^-|_\Sigma$. The quantity S^i_j is the surface stress-energy tensor at the junction surface Σ; n^μ is the unit normal 4-vector to Σ; and $e^\mu_{(i)}$ are the components of the holonomic basis vectors tangent to Σ (see Ref. [32] for details). Note the dependency of the conservation identity on the stress-energy tensor $T_{\mu\nu}$, and the right-hand side of the conservation identity may also be written as $S^i_{\tau|i} = -[\dot{\sigma} + 2\dot{a}(\sigma + \mathcal{P})/a]$. The momentum flux term, i.e., $[T_{\mu\nu}e^\mu_{(j)}n^\nu]^+_-$, corresponds to the net discontinuity in the momentum flux $F_\mu = T_{\mu\nu}U^\nu$, which impinges on the shell. The conservation identity is a statement that all energy and momentum that plunges into the thin shell, gets caught by the latter, and converts into conserved energy and momentum of the surface stresses of the junction. Now, it may be that the topology change is sufficiently violent to destabilize the thin shell. On the other hand, one may also assume that it is sufficiently mild as not to significantly affect the stability of the surface layer.

In analogy to the case outlined in Ref. [22], where the possibility that inflation might provide a natural mechanism for the enlargement of wormholes to macroscopic size was explored, one could imagine that microscopic wormholes originated through a topology change, and due to the accelerated expansion of the Universe, these submicroscopic constructions could naturally be grown to macroscopic dimensions. For instance, in Ref. [46] the evolution of wormholes and ringholes embedded in a background accelerating Universe driven by dark energy, was analyzed. It was shown that the wormhole's size increases by a factor proportional to the scale factor of the Universe, and still increases significantly if the cosmic expansion is driven by phantom energy. The accretion of dark and phantom energy onto Morris-Thorne wormholes [47,48] was further explored, and it was shown that this accretion gradually increases the wormhole throat, which eventually overtakes the accelerated expansion of the Universe, consequently engulfing the entire Universe, and becomes infinite at a time in the future before the Big Rip. This process has been dubbed the ''Big Trip'' [47,48]. However, in the context of the generalized Chaplygin gas, it was shown that the Big Rip may be avoided altogether [49,50]. We refer the reader to Ref. [51] for more recent details on these issues. In summary, we denote these exotic geometries consisting of dark-energy stars (in the phantom regime) and phantom wormholes as phantom stars. The final product of this topological change, namely, phantom wormholes, have far-reaching physical and cosmological implications, as in addition to being used for interstellar shortcuts, an absurdly advanced civilization may manipulate these geometries to induce closed timelike curves, consequently violating causality.

Concerning the geometry of spacetime undergoing quantum fluctuations, this does not seem to be a source of disagreement, but when we turn to the question of whether or not the topology of spacetime undergoes quantum fluctuations, the problem becomes more subtle. It was Wheeler who first conjectured that spacetime could be subjected to a topology fluctuation at the Planck scale. This means that spacetime undergoes a deep and rapid transformation in its structure. The changing spacetime is best known as spacetime foam, which can be taken as a model for the quantum gravitational vacuum. Some authors have investigated the effects of such a foamy space on the cosmological constant; for instance, one example is the celebrated Coleman mechanism, where wormhole contributions suppress the cosmological constant, explaining its small observed value [52]. Nevertheless, how to realize such a foam-like space and also whether this represents the real quantum gravitational vacuum are still unknown. We can mention some results about topological constraints on the classical evolution of general relativistic spacetimes. They are summarized in two points [27]:

(1) In causally well-behaved classical spacetimes the topology of space does not change as a function of time.
(2) In causally ill-behaved classical spacetimes the topology of space can sometimes change.

From the quantum point of view we can separate the problem of topology change generated by a canonical quantization approach and a functional integral quantization approach. The Hawking topology change theorem is thus enough to show that the topology of space cannot change in canonically quantized gravity [53]. In the Feynman functional integral quantization of gravitation things are different. Indeed, in this formalism, an approach is possible to spacetime foam where we know that fluctuations of topology become an important phenomenon at least at the Planck scale [54]. However, we hasten to add that at the moment it is not clear that such topology changes are completely forbidden. Although there are now promising candidate theories of quantum gravity, it is unknown which, if any, provide the correct methods for calculating properties of quantum spacetime.

ACKNOWLEDGMENTS

F. S. N. L. was funded by Fundação para a Ciência e a Tecnologia (FCT)-Portugal through Grant No. SFRH/BPD/26269/2006.

[1] S. Perlmutter *et al.*, Astrophys. J. **517**, 565 (1999); A. G. Riess *et al.*, Astron. J. **116**, 1009 (1998); Astrophys. J. **607**, 665 (2004); A. Grant *et al.*, Astrophys. J. **560**, 49 (2001); S. Perlmutter, M. S. Turner, and M. White, Phys. Rev. Lett. **83**, 670 (1999); C. L. Bennett *et al.*, Astrophys. J. Suppl. Ser. **148**, 1 (2003); G. Hinshaw *et al.*, arXiv:astro-ph/0302217.

[2] E. J. Copeland, M. Sami, and S. Tsujikawa, Int. J. Mod. Phys. D **15**, 1753 (2006).

[3] T. P. Sotiriou and V. Faraoni, arXiv:0805.1726; S. Nojiri and S. D. Odintsov, Int. J. Geom. Methods Mod. Phys. **4**, 115 (2007); K. Koyama, Gen. Relativ. Gravit. **40**, 421 (2008); F. S. N. Lobo, arXiv:0807.1640.

[4] R. R. Caldwell, Phys. Lett. B **545**, 23 (2002); R. R. Caldwell, M. Kamionkowski, and N. N. Weinberg, Phys. Rev. Lett. **91**, 071301 (2003).

[5] S. Sushkov, Phys. Rev. D **71**, 043520 (2005); O. B. Zaslavskii, Phys. Rev. D **72**, 061303 (2005); P. K. F. Kuhfittig, Classical Quantum Gravity **23**, 5853 (2006); M. Cataldo, P. Labrana, S. del Campo, J. Crisostomo, and

P. Salgado, arxiv:0810.2715.
[6] F. S. N. Lobo, Phys. Rev. D **71**, 084011 (2005); **71**, 124022 (2005).
[7] A. Vikman, Phys. Rev. D **71**, 023515 (2005).
[8] D. F. Mota and C. Van de Bruck, Astron. Astrophys. **421**, 71 (2004); I. Maor, Int. J. Theor. Phys. **46**, 2274 (2007).
[9] F. S. N. Lobo, Classical Quantum Gravity **23**, 1525 (2006).
[10] O. Bertolami and J. Paramos, Phys. Rev. D **72**, 123512 (2005); F. S. N. Lobo, Phys. Rev. D **73**, 064028 (2006).
[11] F. S. N. Lobo, Phys. Rev. D **75**, 024023 (2007).
[12] V. Dzhunushaliev, V. Folomeev, R. Myrzakulov, and D. Singleton, J. High Energy Phys. 07 (2008) 094.
[13] P. O. Mazur and E. Mottola, arXiv:gr-qc/0109035; arXiv: gr-qc/0405111; Proc. Natl. Acad. Sci. U.S.A. **101**, 9545 (2004).
[14] M. Visser and D. L. Wiltshire, Classical Quantum Gravity **21**, 1135 (2004); N. Bilić, G. B. Tupper, and R. D. Viollier, arXiv:astro-ph/0503427; B. M. N. Carter, Classical Quantum Gravity **22**, 4551 (2005); C. Cattoen, T. Faber, and M. Visser, Classical Quantum Gravity **22**, 4189 (2005); F. S. N. Lobo and A. V. B. Arellano, Classical Quantum Gravity **24**, 1069 (2007); A. E. Broderick and R. Narayan, Classical Quantum Gravity**24**, 659 (2007); C. B. M. Chirenti and L. Rezzolla, Classical Quantum Gravity **24**, 4191 (2007); D. Horvat and S. Ilijic, Classical Quantum Gravity **24**, 5637 (2007); P. Rocha, A. Y. Miguelote, R. Chan, M. F. da Silva, N. O. Santos, and A. Wang, arXiv:0803.4200; D. Horvat, S. Ilijic, and A. Marunovic, arXiv:0807.2051.
[15] A. DeBenedictis, D. Horvat, S. Ilijić, S. Kloster, and K. S. Viswanathan, Classical Quantum Gravity **23**, 2303 (2006).
[16] M. A. Abramowicz, W. Kluzniak, and J. P. Lasota, Astron. Astrophys. **396**, L31 (2002).
[17] M. Morris and K. S. Thorne, Am. J. Phys. **56**, 395 (1988).
[18] R. Garattini, Classical Quantum Gravity **22**, 1105 (2005); **24**, 1189 (2007); R. Garattini and F. S. N. Lobo, Classical Quantum Gravity**24**, 2401 (2007).
[19] J. A. Wheeler, Ann. Phys. (N.Y.) **2**, 604 (1957).
[20] J. A. Wheeler, Phys. Rev. **97**, 511 (1955).
[21] J. P. S. Lemos, F. S. N. Lobo, and S. Quinet de Oliveira, Phys. Rev. D **68**, 064004 (2003).
[22] T. A. Roman, Phys. Rev. D **47**, 1370 (1993).
[23] B. Reinhart, Topology **2**, 173 (1963); R. Geroch, J. Math. Phys. (N.Y.) **8**, 782 (1967); G. T. Horowitz, Classical Quantum Gravity **8**, 587 (1991); A. A. Tseytlin, J. Phys. A **15**, L105 (1982); E. Witten, Commun. Math. Phys. **117**, 353 (1988); F. Dowker and S. Surya, Phys. Rev. D **58**, 124019 (1998); H. F. Dowker, R. S. Garcia, and S. Surya, Classical Quantum Gravity **17**, 697 (2000); A. Borde, H. F. Dowker, R. S. Garcia, R. D. Sorkin, and S. Surya, Classical Quantum Gravity **16**, 3457 (1999); A. Anderson and B. DeWitt, Found. Phys. **16**, 91 (1986); S. G. Harris and T. Dray, Classical Quantum Gravity **7**, 149 (1990); R. D. Sorkin, Int. J. Theor. Phys. **36**, 2759 (1997).
[24] D. Hochberg and T. W. Kephart, Phys. Rev. D **47**, 1465 (1993).
[25] V. Dzhunushaliev, arXiv:0809.0957.
[26] M. S. Morris, K. S. Thorne, and U. Yurtsever, Phys. Rev. Lett. **61**, 1446 (1988).
[27] M. Visser, *Lorentzian Wormholes: From Einstein to Hawking* (American Institute of Physics, New York, 1995).
[28] V. Dzhunushaliev and V. Folomeev, arXiv:0711.2840.
[29] F. S. N. Lobo, arXiv:0710.4474.
[30] A. V. B. Arellano and F. S. N. Lobo, Classical Quantum Gravity **23**, 5811 (2006).
[31] A. DeBenedictis and A. Das, Nucl. Phys. **B653**, 279 (2003); N. Furey and A. DeBenedictis, Classical Quantum Gravity **22**, 313 (2005); F. S. N. Lobo, Phys. Rev. D **75**, 064027 (2007); Classical Quantum Gravity **25** 175006 (2008).
[32] F. S. N. Lobo and P. Crawford, Classical Quantum Gravity **22**, 4869 (2005).
[33] J. P. S. Lemos and F. S. N. Lobo, Phys. Rev. D **69**, 104007 (2004); F. S. N. Lobo, Classical Quantum Gravity **21**, 4811 (2004); Gen. Relativ. Gravit. **37**, 2023 (2005).
[34] P. K. F. Kuhfittig, arXiv:0707.4665.
[35] M. R. Mbonye and D. Kazanas, Phys. Rev. D **72**, 024016 (2005).
[36] I. Dymnikova, Int. J. Mod. Phys. D **12**, 1015 (2003).
[37] A. Das, A. DeBenedictis, and N. Tariq, J. Math. Phys. (N.Y.) **44**, 5637 (2003).
[38] R. Arnowitt, S. Deser, and C. W. Misner, in *Gravitation: An Introduction to Current Research* edited by L. Witten (John Wiley & Sons, Inc., New York, 1962).
[39] S. W. Hawking and G. T. Horowitz, Classical Quantum Gravity **13**, 1487 (1996).
[40] J. D. Brown and J. W. York, Jr., Phys. Rev. D **47**, 1420 (1993).
[41] V. P. Frolov and E. A. Martinez, Classical Quantum Gravity **13**, 481 (1996).
[42] E. A. Martinez, Phys. Rev. D **51**, 5732 (1995).
[43] R. Garattini, TSPU Vestnik **44N7**, 72 (2004).
[44] R. Garattini, J. Phys. Conf. Ser. **33**, 215 (2006).
[45] Actually, in Eq. (69), the argument of the log has an absolute value.
[46] P. F. González-Díaz, Phys. Rev. D **68**, 084016 (2003).
[47] P. F. González-Díaz, Phys. Rev. Lett. **93**, 071301 (2004).
[48] P. F. González-Díaz and J. A. J. Madrid, Phys. Lett. B **596**, 16 (2004).
[49] P. F. González-Díaz, Phys. Rev. D **68**, 021303(R) (2003).
[50] J. A. J. Madrid, Phys. Lett. B **634**, 106 (2006).
[51] A. V. Yurov, P. Martin Moruno, and P. F. Gonzalez-Diaz, Nucl. Phys. **B759**, 320 (2006); P. Martin-Moruno, Phys. Lett. B **659**, 40 (2008).
[52] S. R. Coleman, Nucl. Phys. **B310**, 643 (1988).
[53] S. W. Hawking, Phys. Rev. D **46**, 603 (1992).
[54] S. W. Hawking, Phys. Rev. D **18**, 1747 (1978).